

Article

5-Aryl-1-Arylideneamino-1*H*-Imidazole-2(3*H*)-Thiones: Synthesis and In Vitro Anticancer Evaluation

Ali H. Abu Almaaty ¹, Eslam E. M. Toson ², El-Sherbiny H. El-Sayed ², Mohamed A. M. Tantawy ³, Eman Fayad ⁴, Ola A. Abu Ali ⁵ and Islam Zaki ^{6,*}

¹ Zoology Department, Faculty of Science, Port Said University, Port Said 42526, Egypt; ali_zoology_2010@yahoo.com

² Chemistry Department, Faculty of Science, Port Said University, Port Said 42526, Egypt; eslamatwa2010@gmail.com (E.E.M.T.); saeed201691@yahoo.com (E.-S.H.E.-S.)

³ Medical Research Division, National Research Centre, Dokki, Giza 12511, Egypt; mohamed_tantawy@daad-alumni.de

⁴ Biotechnology Department, Faculty of Science, Taif University, P.O. Box 11099, Taif 21944, Saudi Arabia; e.esmail@tu.edu.sa

⁵ Chemistry Department, College of Science, Taif University, P.O. Box 11099, Taif 21944, Saudi Arabia; O.abuali@tu.edu.sa

⁶ Pharmaceutical Organic Chemistry Department, Faculty of Pharmacy, Port Said University, Port Said 42526, Egypt

* Correspondence: eslam.zaki@pharm.psu.edu.eg; Tel.: +20-1153436140

Abstract: A novel series of *N*-1 arylidene amino imidazole-2-thiones were synthesized, identified using IR, ¹H-NMR, and ¹³C-NMR spectral data. Cytotoxic effect of the prepared compounds was carried out utilizing three cancer cell lines; MCF-7 breast cancer, HepG2 liver cancer, and HCT-116 colon cancer cell lines. Imidazole derivative **5** was the most potent of all against three cell lines. DNA flow cytometric analysis showed that, imidazoles **4d** and **5** exhibit pre-G1 apoptosis and cell cycle arrest at G2/M phase. The results of the VEGFR-2 and B-Raf kinase inhibition assay revealed that compounds **4d** and **5** displayed good inhibitory activity compared with reference drug erlotinib.

Keywords: imidazole; synthesis; cytotoxicity; apoptosis; cell cycle analysis; Annexin V; VEGFR-2



Citation: Abu Almaaty, A.H.; Toson, E.E.M.; El-Sayed, E.-S.H.; Tantawy, M.A.M.; Fayad, E.; Abu Ali, O.A.; Zaki, I. 5-Aryl-1-Arylideneamino-1*H*-Imidazole-2(3*H*)-Thiones: Synthesis and In Vitro Anticancer Evaluation. *Molecules* **2021**, *26*, 1706. <https://doi.org/10.3390/molecules26061706>

Academic Editor: René Csuk

Received: 8 February 2021

Accepted: 15 March 2021

Published: 18 March 2021

Publisher's Note: MDPI stays neutral with regard to jurisdictional claims in published maps and institutional affiliations.



Copyright: © 2021 by the authors. Licensee MDPI, Basel, Switzerland. This article is an open access article distributed under the terms and conditions of the Creative Commons Attribution (CC BY) license (<https://creativecommons.org/licenses/by/4.0/>).

1. Introduction

Cancer is the pathological uncontrolled proliferation of the abnormal cells that divide rapidly [1]. Moreover, cancer can involve any tissue of the body and have many different forms in each body area [2,3]. Therefore, there is a constant and growing interest to synthesize new biologically active molecules which might be useful in a cancer treatment.

Anticancer activity of the azole derivatives is most extensively studied and some of them are in clinical practice as antitumor active agents [4,5]. Imidazoles are an important class of heterocyclic molecules and imidazole derivatives are reported to have anticancer activity [6–8]. Misonidazole **I** displayed superior antiproliferative activity against a panel of cancer cell lines [9]. Tiazofurin **II** possesses good anticancer activity [10]. Lepidiline A and B are imidazole compounds which exhibit cytotoxicity against various types of human cancer cell lines at micromolar concentration [11]. Imidazole derivatives were found to exert their anticancer activity by acting mainly as antiangiogenic agents, inhibitors of B-Raf kinase, and as p38 MAP kinase inhibitors [12–14]. For example, compound **III** displayed potent antitumor activity against the MCF-7 cell line with an IC₅₀ value of 3.26 μM, as compared with SOR (IC₅₀ = 1.12 μM) [15]. Additionally, compound **IV** has been reported as a vascular endothelium growth factor (VEGFR-2) inhibitor and apoptotic inducer [15]. Moreover, it has been reported that imidazole molecule **V** inhibits the kinase activity of Raf in low nanomolar concentrations [16]. Furthermore, compound **VI** was identified as a submicromolar inhibitor of B-Raf kinase [17] (Figure 1).

Based on the aforementioned aspects, the present study is concerned with the synthesis of novel imidazole molecules bearing arylidene amino substituents at the *N*-1 position. It is worthy to note that imidazole fragments are decorated at the C-5 position with phenyl groups carrying chloro or methoxy substituents to show the impact on anticancer activity. Finally, full details about the synthesis and evaluation of the antitumor activity *in vitro* are reported herein.

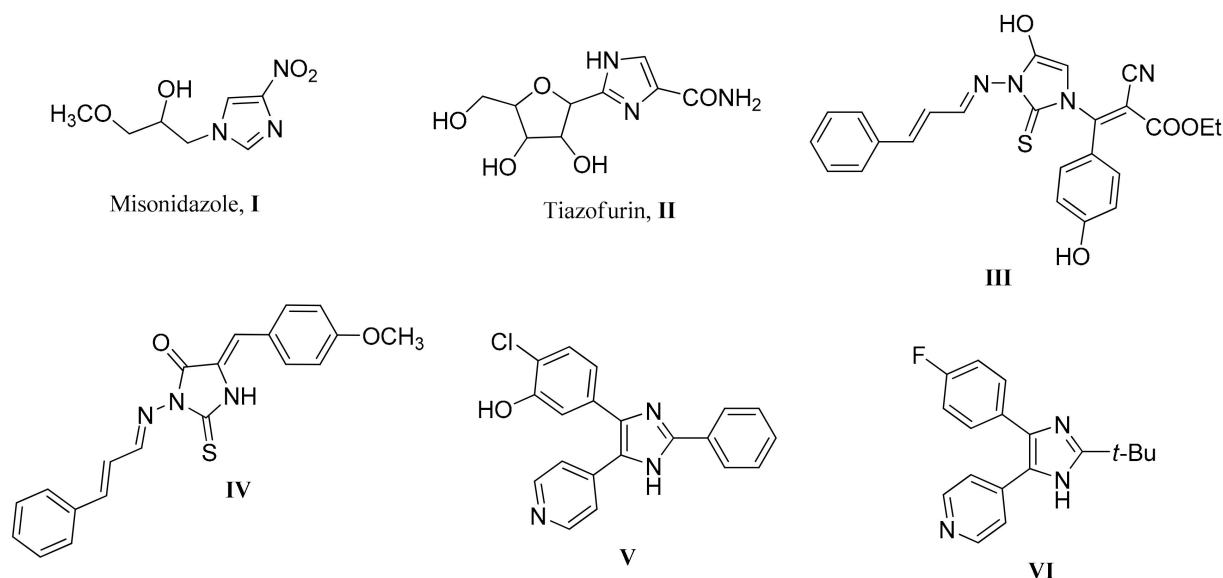


Figure 1. Imidazole derivatives as anticancer agents.

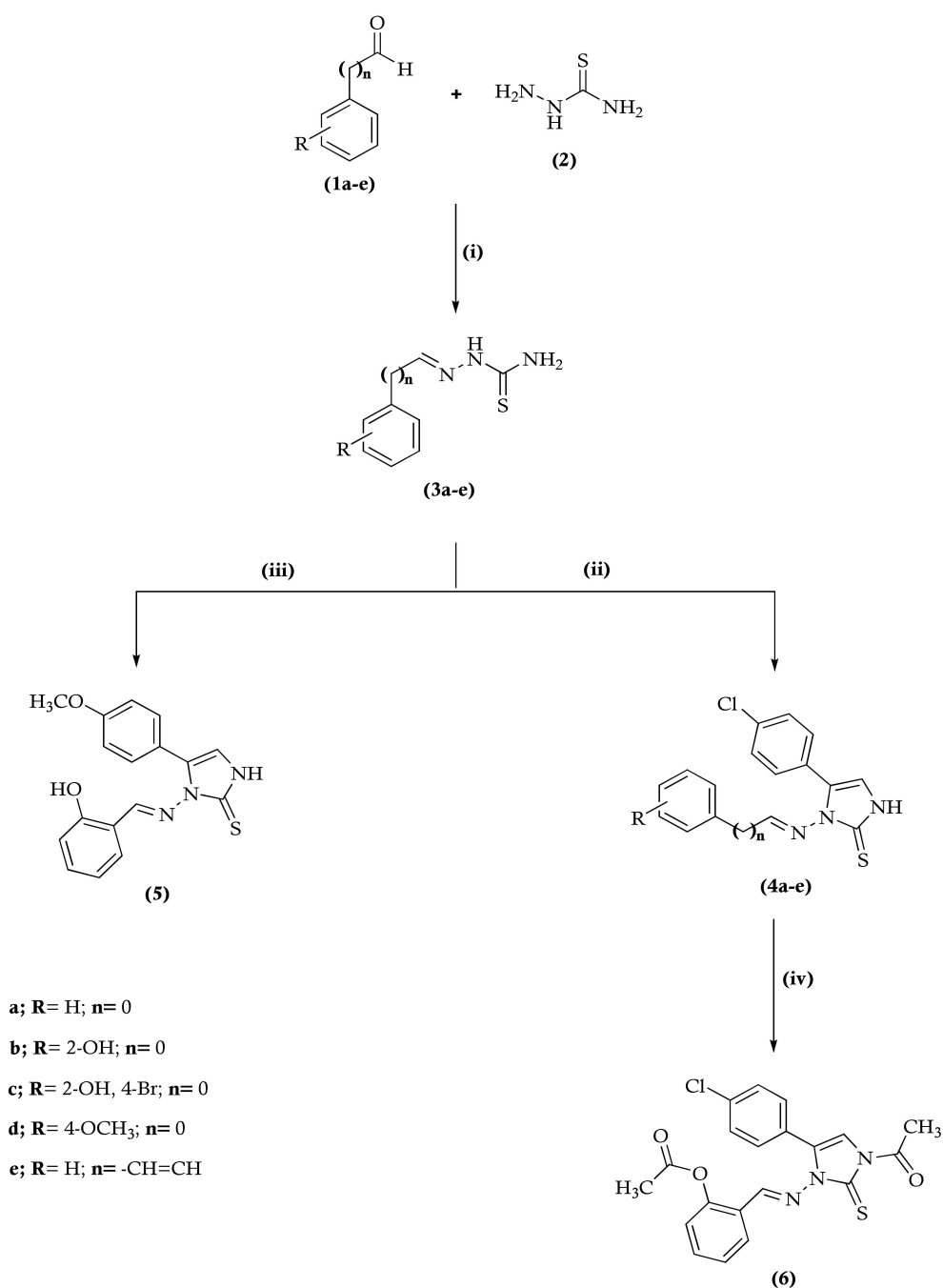
2. Result and Discussion

2.1. Chemistry

2-Arylhiazinecarbothioamides **3a–e** were prepared in high yield according to the reported procedure [18,19] through condensation of aromatic aldehydes (namely, benzaldehyde, 2-hydroxybenzaldehyde, 5-bromo-2-hydroxybenzaldehyde, 4-methoxybenzaldehyde, 4-hydroxy-3-methoxybenzaldehyde, and cinnamaldehyde) with thiosemicarbazide in refluxing ethanol containing catalytic amounts of acetic acid. The structure of **3a–e** was confirmed using different spectroscopic techniques. The $^1\text{H-NMR}$ spectra revealed the presence of a signal for a azomethine group ($\text{CH}=\text{N}$) at δ 7.92–8.38 ppm. In addition to new signals attributed to NH and NH_2 groups. Carbon signals observed in $^{13}\text{C-NMR}$ spectra at δ 140.10–145.19 and 178.01–178.10 ppm assigned to carbons of azomethine ($\text{CH}=\text{N}$) and thiocarbonyl ($\text{C}=\text{S}$) groups, respectively, confirmed formation of 2-arylhiazinecarbothioamides **3a–e**.

Furthermore, the novel imidazole derivatives **4a–e** and **5** were synthesized by cyclocondensation of 2-arylhiazinecarbothioamides **3a–e** and substituted phenacylbromide in absolute ethanol in the presence of fused sodium acetate under reflux temperature (Scheme 1). The structure of novel imidazoles **4a–e** was characterized using different spectroscopic methods. The $^1\text{H-NMR}$ spectra revealed the presence of additional aromatic signals attributed to phenyl ring B protons.

Compound **4b**, as a representative example, was established chemically via an acetylation reaction with acetic anhydride, which gave 2-((3-acetyl-5-(4-chlorophenyl)-2-thioxo-2,3-dihydro-1*H*-imidazol-1-ylimino)methyl)phenyl acetate (**6**), Scheme 1. The $^1\text{H-NMR}$ spectrum of compound **6** showed the absence NH signals, and OH groups with the appearance of two new singlet signals at δ 2.08, 2.51, and 2.54 ppm due to the protons of two methyl function of acetyl groups. The $^{13}\text{C-NMR}$ spectrum of compound **6** showed the presence of four new carbon signals at δ 20.02, 22.95, 169.50, and 172.13 related to two acetyl groups (CH_3CO) which supported the formation of compound **6**.



Scheme 1. Synthesis of imidazole-2-thione derivatives **4a–f**, **5** and **6**. Reagents and reaction condition: (i) EtOH, AcOH, reflux; (ii) 4-chlorophenacylbromide, NaOAc, EtOH; (iii) 4-methoxyphenacylbromide, NaOAc, EtOH; (iv) Ac₂O, reflux.

2.2. In Vitro Antitumor Evaluation

2.2.1. In Vitro Cytotoxic Activity against Three Cancer Cell Lines

The effect of imidazole molecules **4a–e** and **5** on the viability of three cancer cell lines were studied using the MTT assay. The cytotoxicity was assessed using Docetaxel (DOC) as a standard antitumor drug. The three cancer cell lines were MCF-7 (breast cancer cell line), colon carcinoma (HCT-116), and HepG2 (hepatocellular carcinoma cell line). Treatment of MCF-7, HCT-116, and HepG2 cell lines with different concentrations of imidazole derivatives revealed moderate to good antitumor activities as concluded from their IC₅₀ values shown in Table 1. Compound 1-(2-hydroxybenzylideneamino)-5-(4-methoxyphenyl)-1*H*-imidazole-2(3*H*)-thione (**5**) was the most potent cytotoxic compound against all of the tested tumor cell lines with IC₅₀s < 5 μM. Moreover, the safety of

compounds **4d** and **5** was assessed against a normal breast cell line (MCF-10A) using the MTT assay. The results revealed weak cytotoxic effect towards MCF-10A and compound **4d** showed less cytotoxic effect than standard drug DOC.

Table 1. In vitro IC₅₀ values (μM) of imidazole derivatives **4a–e** and **5** over MCF-7, HepG2, HCT-116, and MCF-10A cell lines. Data are expressed as the mean ± three experiments.

Comp No.	IC ₅₀ (μM)			
	MCF-7	HepG2	HCT-116	MCF-10A
4a	>50	61.81 ± 4.1	20.56 ± 1.4	NT
4b	24.94 ± 1.6	>50	23.53 ± 1.6	NT
4c	43.95 ± 2.9	11.36 ± 0.8	9.962 ± 0.7	NT
4d	7.967 ± 0.5	4.086 ± 0.3	28.95 ± 1.9	44.06 ± 0.23
4e	13.15 ± 0.9	17.01 ± 1.1	3.988 ± 0.3	NT
5	1.071 ± 0.1	1.301 ± 0.1	3.99 ± 0.3	27.81 ± 0.31
DOC	11.09 ± 0.7	8.128 ± 0.5	13.96 ± 0.9	33.17 ± 0.19

NT; not tested.

2.2.2. Cell Cycle Analysis

The most active compounds, **4d** and **5** on MCF-7 were studied using DNA flow cytometric analysis. Treatment of MCF-7 cells with IC₅₀ concentration dose value of compounds **4d** and **5** resulted in a significant alteration in cell cycle profile. There was a significant increase in the percentage of cell population at the G2/M phase from (8.79%) control to 35.55% and 25.63% upon treatment with compounds **4d** and **5**, respectively. Additionally, a significant increase in the percentage of cells at pre-G1 phase from 1.61% (control) to 22.36% and 22.81% upon treatment with compounds **4d** and **5**, respectively. Therefore, it can be concluded that compounds **4d** and **5** inhibit the cell proliferation of MCF-7 cells via cell cycle arrest at the G2/M phase and induction of apoptosis (Figure 2).

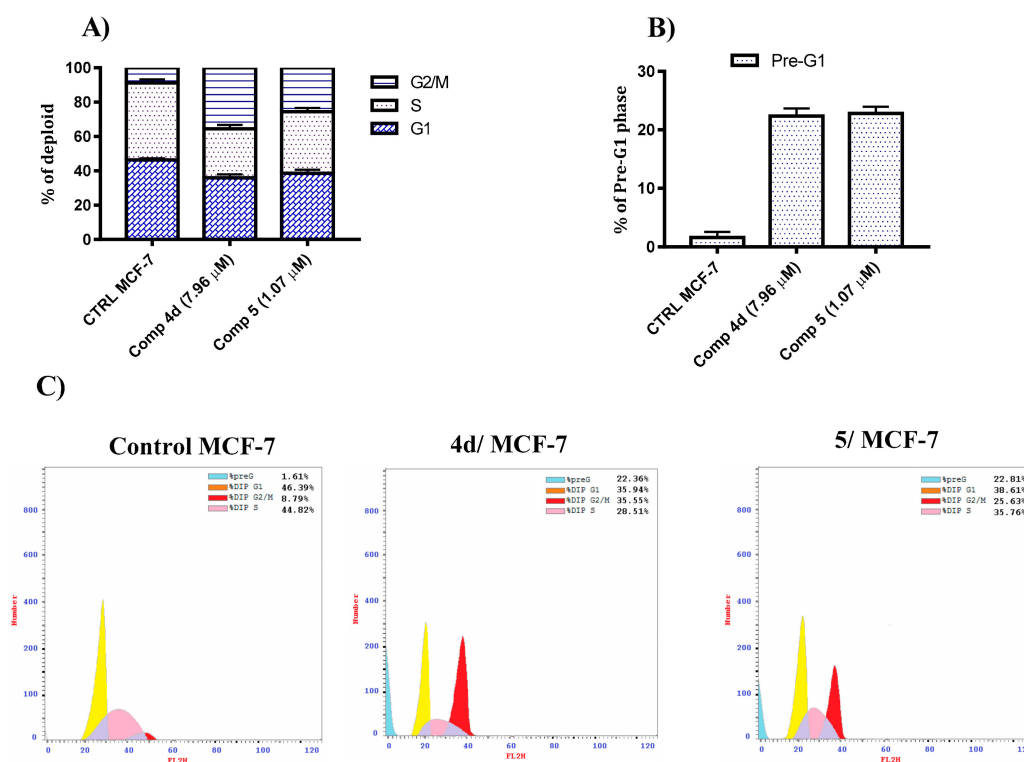


Figure 2. (A) A graphical representation of cell cycle analysis of compounds **4d** and **5** against MCF-7 at their IC₅₀ (μM). (B) A graphical representation of the percentage of pre-G1 phase induced by compounds **4d** and **5** against MCF-7 at their IC₅₀ (μM). (C) Cell cycle analysis of compounds **4d** and **5** against MCF-7 at their IC₅₀ (μM).

2.2.3. Annexin V-FITC/PI Apoptosis Induction Analysis

Several imidazole molecules have been reported in the literature as apoptosis inducers in several tumor cell lines [20]. To evaluate the mode of cell death induced by compounds **4d** and **5**, Annexin V/FITC and propidium iodide (PI) assays were performed. MCF-7 cells were treated with compounds **4d** and **5** at their IC_{50} concentration dose value for 48 h. The results showed that the selected candidates induce apoptosis of MCF-7 cells at both early and later stages. As shown in Figure 3, the percent of early apoptosis was increased from 0.43% (control) to 6.12% and 2.66% for compounds **4d** and **5**, respectively. Additionally, the percent of late apoptosis was increased from 0.23% (control) to 10.23% and 13.64% upon exposure to compounds **4d** and **5**, respectively. The results proved that the antiproliferative activity of compounds **4d** and **5** is attributed to its apoptosis inducing activity in MCF-7 cells.

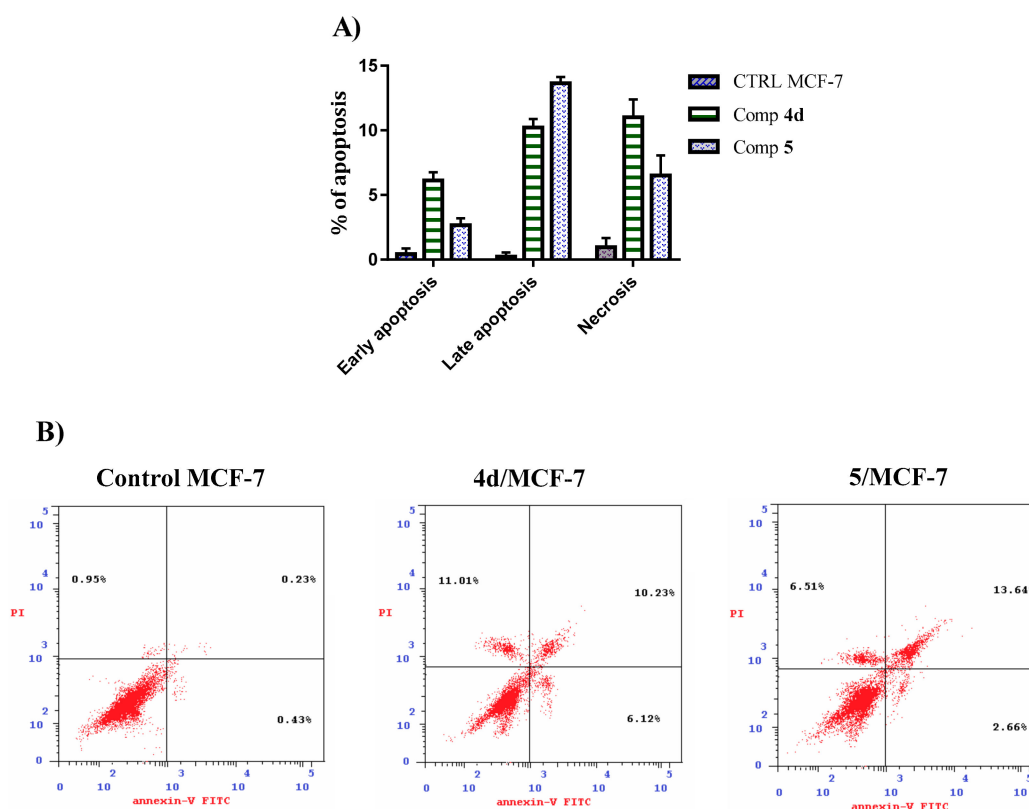


Figure 3. (A) A graphical representation of apoptosis induction analysis of compounds **4d** and **5** against MCF-7 at their IC_{50} (μ M). (B) Apoptosis induction analysis of compounds **4d** and **5** against MCF-7 at their IC_{50} (μ M).

2.2.4. VEGFR-2 Kinase Inhibitory Activity

To investigate the possible molecular mechanism underlying the potent anticancer activity of compounds **4d** and **5**. Their inhibitory activity against VEGFR-2 kinase was determined using an ELISA assay. The results in (Figure 4) showed that the selected imidazole molecules **4d** and **5** elicited potent activity against VEGFR-2 kinase with IC_{50} values 247.81 and 82.09 ng/mL, respectively, compared with erlotinib as the reference drug. According to these results, imidazole molecules **4d** and **5** possess good inhibition of VEGFR-2 kinase activity.

2.2.5. B-Raf Inhibitory Activity

Raf is a protein kinase that initiates a cascade of other protein kinases by acting on the protein kinases MEK-1 and MEK-2 [21]. Therefore, constitutive activation of this signaling pathway is observed in variety of cancers. In the present assay, the activity potential of compounds **4d** and **5** was evaluated against B-Raf^{V600E} using an ELISA assay.

The results showed that compounds **4d** and **5** revealed good inhibitory activities against B-Raf^{V600E} with IC₅₀ values of 13.05 and 2.38 µg/mL, respectively, compared with the value of 0.98 µg/mL for erlotinib (Figure 5).

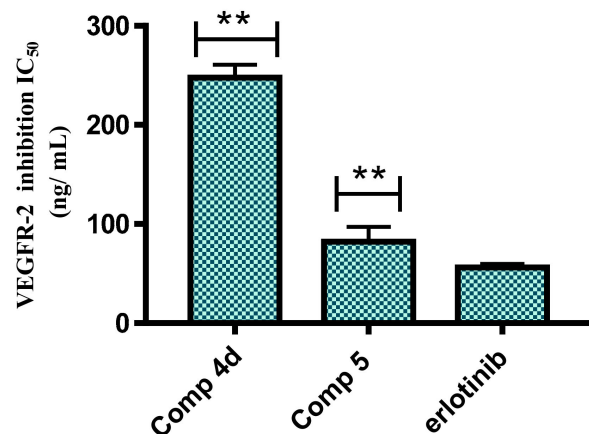


Figure 4. A graphical representation of the IC₅₀ values (ng/mL) of compounds **4d**, **5**, and erlotinib for the VEGFR-2 enzyme. Data are expressed as the mean ($n = 3$ experiments) \pm SEM and statistical comparisons were carried out using one-way analysis of variance (ANOVA) followed by Tukey's multiple comparisons test (**, $p < 0.05$).

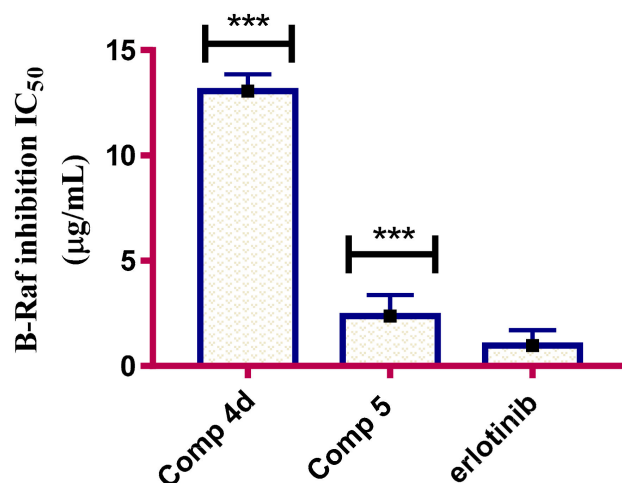


Figure 5. A graphical representation of the IC₅₀ values (µg/mL) of compounds **4d**, **5**, and erlotinib for the B-Raf enzyme. Data are expressed as mean ($n = 3$ experiments) \pm SEM and statistical comparisons were carried out using one-way analysis of variance (ANOVA) followed by Tukey's multiple comparisons test (***, $p < 0.005$).

2.2.6. Molecular Docking Study

Compounds **4d** and **5** were docked into the VEGFR-2 crystal structure (PDB code: 3U6J) [22]. Compound **4d** interacted with the active site of 3U6J by hydrogen bonding with the amino acid Lys 868 by its methoxy group. In addition, the hydrophobicity induced by compound **4d** resulted in a docking score of -20.69 kcal/mol. On the other hand, compound **5** interacted through hydrogen bonding with the amino acids Lys 868 and Ile 1025 by its methoxy and hydroxy groups, respectively, and its hydrophobicity resulted in docking score of -21.58 kcal/mol (Figure 6). The interaction result is consistent with the obtained IC₅₀ values against the VEGFR-2 enzyme. Accordingly, from the obtained results, compound **5** was more potent than compound **4d** and with higher VEGFR-2 inhibitory activity.

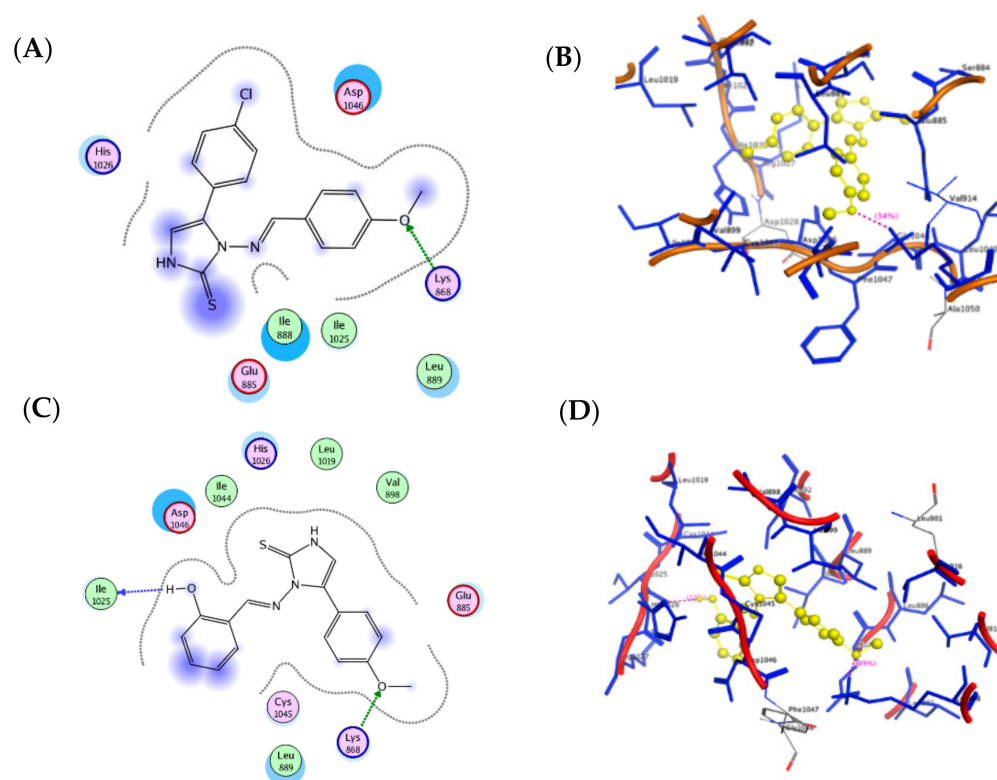


Figure 6. (A) 2D representation of compound **4d** docking inside the active site of 3U6J. (B) 3D representation of compound **4d** docking inside the active site of 3U6J. (C) 2D representation of compound **5** docking inside the active site of 3U6J. (D) 3D representation of compound **5** docking inside the active site of 3U6J.

3. Material and Methods

3.1. General

^1H and ^{13}C -NMR spectra were measured with a Bruker 400 DRX, Avance NMR spectrometer (Chichago, Elk Grove Village, USA) using the DMSO- d_6 solvent. The IR data were obtained with a shimadzu 470 spectrometer (Kyoto, Kyoto, Japan). Melting points of the prepared derivatives were measured with an electro thermal melting point apparatus and were not corrected. The microanalyses were implemented on a Perkin Elmer CHN elemental analyzer (Haan, Germany). All chemicals were purchased from Aldrich chemical company and all reagents were of analytical grade. The prepared imidazole molecules were soluble in DMSO and not soluble in water at any concentration.

3.2. General Procedure for the Synthesis of 2-Arylhydrazinecarbothioamide (**3a–d**)

To a mixture of aromatic aldehyde (0.01 mol) and thiosemicarbazide **2** in absolute ethanol (50 mL) and a few drops of glacial acetic acid were added. The reaction mixture was heated under reflux for 4 h. After cooling, the separated solid was collected by filtration, dried, and crystallized from ethanol to give **3a–d**.

3.2.1. (E)-2-Benzylidenehydrazinecarbothioamide (**3a**)

Pale yellow crystals, yield 83%. m.p. 188–190 °C. IR (KBr) ν_{max} : 3418, 3262, 3154 (NH), 3072 (arom.CH), 1591 (C=N), 1536, 1451 (C=C), 1292 (C=S) cm^{-1} . ^1H -NMR (DMSO- d_6) δ : 7.51–7.35 (m, 3H, arom. CH), 7.81 (dd, $J = 6.4, 3.0$ Hz, 2H, arom. CH), 8.03 (s, 1H, NH), 8.06 (s, 1H, CH=N), 8.24 (s, 1H, NH), 11.47 (s, 1H, NH) ppm. ^{13}C -NMR (DMSO- d_6) δ : 125.52, 127.40, 129.32, 139.34 (C- aromatic), 145.19 (CH=N), 178.10 (C=S) ppm.

3.2.2. (E)-2-(2-Hydroxybenzylidene)hydrazinecarbothioamide (**3b**)

Yellow crystals, yield 81%, m.p. 210–212 °C. IR (KBr) ν_{\max} : 3444 (OH), 3319, 3140 (NH), 3032 (arom.CH), 1613 (C=N), 1539, 1491 (C=C), 1368 (C=S), 1113 (C–O) cm^{-1} . $^1\text{H-NMR}$ (DMSO- d_6) δ : $^1\text{H-NMR}$ (DMSO- d_6) δ : 6.80 (t, $J = 8.4$ Hz, 1H, arom.CH), 6.86 (d, $J = 8.4$ Hz, 1H, arom. CH), 7.20 (t, $J = 8.5$ Hz, 1H, arom.CH), 7.91 (s, 2H, arom.CH and NH), 8.15 (s, 1H, CH=N), 8.38 (s, 1H, NH), 9.90 (br. s, 1H, OH), 11.38 (s, 1H, NH) ppm. $^{13}\text{C-NMR}$ (DMSO- d_6) δ : 116.50, 119.75, 120.80, 127.21, 131.57 (C-aromatic), 140.10 (CH=N), 156.87 (C–O), 178.10 (C=S) ppm.

3.2.3. (E)-2-(4-Methoxybenzylidene)hydrazinecarbothioamide (**3c**)

Yellow crystals, yield 81%, m.p. 192–194 °C. IR (KBr) ν_{\max} : 3404, 3290, 3154 (NH), 1604 (C=N), 1536, 1511 (C=C), 1361 (C=S) cm^{-1} . $^1\text{H-NMR}$ (DMSO- d_6) δ : 3.78 (s, 3H, OCH₃), 6.96 (d, $J = 8.6$ Hz, 2H, arom.CH), 7.74 (d, $J = 8.6$ Hz, 2H, arom.CH), 7.95 (s, 1H, NH), 8.02 (s, 1H, CH=N), 8.16, 11.37 (s, 2H, NH₂) ppm. $^{13}\text{C-NMR}$ (DMSO- d_6) δ : 55.73 (OCH₃), 114.60, 127.17, 129.38 (C-aromatic), 142.72 (CH=N), 161.12 (C–O), 178.01 (C=S) ppm.

3.2.4. (E)-2-((E)-3-Phenylallylidene)hydrazinecarbothioamide (**3d**)

Pale yellow crystals, yield 79 %, m.p. 134–136 °C. IR ν_{\max} : 3418, 3262, 3154 (NH), 3027 (arom.CH), 1591 (C=N), 1536, 1451 (C=C), 1371 (C=S) cm^{-1} . $^1\text{H-NMR}$ (DMSO- d_6) δ : 6.88 (dd, $J = 16.1, 9.2$ Hz, 1H olefinic CH), 7.03 (d, $J = 16.1$ Hz, 1H, olefinic CH), 7.45–7.34 (m, 3H, arom.CH), 7.57 (d, $J = 7.2$ Hz, 2H, arom.CH), 7.68 (s, 1H, NH), 7.92 (d, $J = 9.2$ Hz, 1H, CH=N), 8.22, 11.44 (s, 2H, NH₂) ppm. $^{13}\text{C-NMR}$ (DMSO- d_6) δ : 119.12, 125.52, 127.40, 129.32, 136.32, 139.34 (C-aromatic and olefinic), 145.19 (CH=N), 178.10 (C=S) ppm.

3.3. General Procedure for the Synthesis of Imidazole Derivatives **4a–e** and **5**

A suspension of thiosemicarbazone derivative **3a–e** (0.01 mol) and freshly prepared substituted phenacyl bromide (0.01 mol) in 30 mL of absolute ethanol and freshly fused sodium acetate (0.03 mol) was refluxed for 6 h. After concentration and cooling, the solid that formed was collected and crystallized from proper solvent to give the target imidazole compound.

3.3.1. (E)-1-(Benzylideneamino)-5-(4-chlorophenyl)-1H-imidazole-2(3H)-thione (**4a**)

Pale yellow crystals, yield 78%, m.p. 121–123 °C crystallized from dioxane; IR (KBr) ν_{\max} : 3403 (NH), 3109 (arom.CH), 1604 (C=N), 1566, 1512 (C=C), 1255 (C=S) cm^{-1} . $^1\text{H-NMR}$ (DMSO- d_6) δ : 7.32 (s, 1H, H-4 of imidazole ring), 7.48–7.38 (m, 5H, arom.CH), 7.64 (d, $J = 7.1$ Hz, 2H, arom.CH), 7.85 (d, $J = 8.5$ Hz, 2H, arom.CH), 8.04 (s, 1H, CH=N), 12.12 (s, 1H, NH) ppm. $^{13}\text{C-NMR}$ (DMSO- d_6) δ : 104.93 (C4 imidazole), 126.71 (C2,6 chlorophenyl), 127.67 (C3,5 chlorophenyl), 129.10 (C3,5 phenyl), 129.33 (C2,6 phenyl), 129.87 (C4 imidazole), 132.45 (C4 phenyl), 133.84 (C1 chlorophenyl), 134.68 (C4 chlorophenyl), 142.02 (C4 phenyl), 149.75 (C=N), 178.27 (C=S) ppm. Anal. Calcd for C₁₆H₁₂ClN₃S (313.80). Calculated: C, 61.24; H, 3.85; N, 13.39. Found: C, 61.12; H, 3.61; N, 13.48.

3.3.2. (E)-5-(4-Chlorophenyl)-1-(2-hydroxybenzylideneamino)-1H-imidazole-2(3H)-thione (**4b**)

Yellow crystals, yield 79 %, m.p. 128–130 °C; crystallized from ethanol/ H₂O (3:1); IR (KBr) ν_{\max} : 3442 (OH), 3315 (NH), 3039 (arom.CH), 1614 (C=N), 1578. 1540 (C=C), 1267 (C=S), 1092 (C–O) cm^{-1} . $^1\text{H-NMR}$ (DMSO- d_6) δ : 6.95–6.88 (m, 2H, arom.CH), 7.29–7.18 (m, 2H, arom.CH), 7.40 (s, 1H, H-4 of imidazole ring), 7.48 (d, $J = 8.5$ Hz, 2H, arom.CH), 7.88 (d, $J = 8.5$ Hz, 2H, arom.CH), 8.35 (s, 1H, CH=N), 10.14 (s, 1H, OH), 12.18 (s, 1H, NH) ppm. $^{13}\text{C-NMR}$ (DMSO- d_6) δ : 104.64 (C4 imidazole), 116.61 (C3 hydroxyphenyl), 119.08 (C1 hydroxyphenyl), 120.83 (C5 hydroxyphenyl), 127.71 (C2,6 chlorophenyl), 129.12 (C3,5 chlorophenyl), 131.06 (C6 hydroxyphenyl), 131.55 (C5 imidazole), 132.43 (C1 chlorophenyl), 133.93 (C4 hydroxyphenyl), 139.98 (C4 chlorophenyl), 149.76 (C=N), 156.41 (C2 hydroxyphenyl), 178.08 (C=S) ppm. Anal. Calcd for C₁₆H₁₂ClN₃OS (329.80). Calculated: C, 58.27; H, 3.67; N, 12.74. Found: C, 58.41; H, 3.89; N, 12.49.

3.3.3. (E)-1-(5-Bromo-2-hydroxybenzylideneamino)-5-(4-chlorophenyl)-1H-imidazole-2(3H)-thione (4c)

Yellow crystals, yield 78%, m.p. 191–193 °C; crystallized from ethanol/ H₂O (3:1); IR (KBr) ν_{\max} : 3454 (OH), 3252 (NH), 3059 (arom.CH), 1592 (C=N), 1548, 1477 (C=C), 1263 (C=S), 1086 (C–O) cm⁻¹. ¹H-NMR (DMSO-*d*₆) δ : 6.89 (d, *J* = 8.7 Hz, 1H, arom.CH), 7.35 (d, *J* = 8.7 Hz, 1H, arom.CH), 7.41 (s, 1H, H-4 of imidazole ring), 7.47 (d, *J* = 8.5 Hz, 2H, arom.CH), 7.77 (s, 1H, arom.CH), 7.88 (d, *J* = 8.5 Hz, 2H, arom.CH), 8.27 (s, 1H, CH=N), 10.41 (s, 1H, OH), 12.29 (s, 1H, NH) ppm. ¹³C-NMR (DMSO-*d*₆) δ : 104.93 (C4 imidazole), 111.29 (C5 bromohydroxyphenyl), 118.87 (C3 bromohydroxyphenyl), 123.19 (C1 bromohydroxyphenyl), 127.70 (C2,6 chlorophenyl), 129.11 (C3,5 chlorophenyl), 132.45 (C5 imidazole and C6 bromohydroxyphenyl), 133.15 (C1,4 chlorophenyl), 137.50 (C4 bromohydroxyphenyl), 149.85 (C=N), 155.47 (C2 bromohydroxyphenyl), 178.28 (C=S) ppm. Anal. Calcd for C₁₆H₁₁BrClN₃OS (408.70). Calculated: C, 47.02; H, 2.71; N, 10.28. Found: C, 46.89; H, 2.57; N, 10.43.

3.3.4. (E)-5-(4-Chlorophenyl)-1-(4-methoxybenzylideneamino)-1H-imidazole-2(3H)-thione (4d)

Yellow crystals, yield 81%, m.p. 151–153 °C; crystallized from ethanol/H₂O (3:1); IR (KBr) ν_{\max} : 3422 (NH), 3033 (arom.CH), 1575 (C=N), 1477, 1426 (C=C), 1352 (C=S), 1092 (C–O) cm⁻¹. ¹H-NMR (DMSO-*d*₆) δ : 3.78 (s, 3H, OCH₃), 6.98 (d, *J* = 8.8 Hz, 2H, arom.CH), 7.34 (s, 1H, H-4 of imidazole ring), 7.44 (d, *J* = 8.6 Hz, 2H, arom.CH), 7.59 (d, *J* = 8.8 Hz, 2H, arom.CH), 7.86 (d, *J* = 8.6 Hz, 2H, arom.CH), 7.99 (s, 1H, C=N), 12.04 (s, 1H, NH) ppm. ¹³C-NMR (DMSO-*d*₆) δ : 55.71 (OCH₃), 104.621 (C4 imidazole), 114.80 (C3,5 methoxyphenyl), 127.43 (C1 methoxyphenyl), 127.66 (C2,6 chlorophenyl), 128.29 (C3,5 chlorophenyl), 129.07 (C2,6 methoxyphenyl), 132.34 (C5 imidazole), 134.05 (C1 chlorophenyl), 141.88 (C4 chlorophenyl), 142.68 (CH=N), 160.72 (C4 methoxyphenyl), 178.25 (C=S) ppm. Anal. Calcd for C₁₇H₁₄ClN₃OS (343.83). Calculated: C, 59.38; H, 4.10; N, 12.22. Found: C, 59.29; H, 3.89; N, 12.06.

3.3.5. 5-(4-Chlorophenyl)-1-((E)-((E)-3-phenylallylidene)amino)-1H-imidazole-2(3H)-thione (4e)

Pale yellow crystals, yield 78%, m.p. 139–141 °C crystallized from dioxane; IR (KBr) ν_{\max} : 3499 (NH), 3059 (arom.CH), 1683 (C=N), 1565, 1480 (C=C), 1259 (C=S) cm⁻¹. ¹H-NMR (DMSO-*d*₆) δ : 6.94 (s, 1H, H-4 of imidazole ring), 7.02–7.04 (m, 1H, olefinic CH), 7.30 (d, *J* = 7.3 Hz, 1H, olefinic CH), 7.38–7.32 (m, 3H, arom.CH), 7.46 (d, *J* = 8.6 Hz, 2H, arom.CH), 7.58 (d, 2H, arom.CH), 7.88 (d, *J* = 10.1, 3.3 Hz, 2H, arom.CH), 7.93 (d, *J* = 4.1 Hz, 1H, CH=N), 12.16 (s, 1H, NH) ppm. ¹³C-NMR (DMSO-*d*₆) δ : 104.81 (C4 imidazole), 125.63 (C2 allylidene), 127.36 (C2,6 chlorophenyl), 127.68 (C2,6 phenyl), 129.08 (C3,5 phenyl), 129.23 (C3,5 chlorophenyl), 130.49 (C4 phenyl), 132.45 (C5 imidazole), 133.98 (C1 chlorophenyl), 136.60 (C3 allylidene), 137.22 (C4 chlorophenyl), 144.59 (C1 phenyl), 149.80 (C=N), 178.16 (C=S) ppm. Anal. Calcd for C₁₈H₁₄ClN₃S (339.84). Calculated: C, 63.62; H, 4.15; N, 12.36. Found: C, 63.53; H, 4.01; N, 12.12.

3.3.6. (E)-1-(2-Hydroxybenzylideneamino)-5-(4-methoxyphenyl)-1H-imidazole-2(3H)-thione (5)

Yellow crystals, yield 76.40%, m.p. IR (KBr) ν_{\max} : 3442 (OH), 3319 (NH), 3032 (arom.CH), 2986 (aliph.CH), 1613 (C=N), 1540, 1489 (C=C), 1271 (C=S), 1203, 1056 (C–O) cm⁻¹. ¹H-NMR (DMSO-*d*₆) δ : 3.89 (s, 3H, OCH₃), 6.92–6.80 (m, 3H, arom.CH), 7.17 (d, *J* = 8.8 Hz, 1H, arom.CH), 7.22 (d, *J* = 8.8 Hz, 1H, arom.CH), 7.31 (s, 1H, H-4 of imidazole ring), 7.64 (d, *J* = 6.7 Hz, 1H, arom.CH), 7.94 (d, *J* = 6.3 Hz, 2H, arom.CH), 8.39 (s, 1H, CH=N), 9.91 (s, 1H, OH), 11.41 (s, 1H, NH) ppm. ¹³C-NMR (DMSO-*d*₆) δ : 56.76 (OCH₃), 102.99 (C4 imidazole), 111.25 (C3 hydroxyphenyl), 113.20 (C1 hydroxyphenyl), 116.47 (C5 hydroxyphenyl), 119.72 (C3,5 methoxyphenyl), 127.17 (C1 methoxyphenyl), 130.41 (C6 hydroxyphenyl), 131.05 (C5 imidazole), 131.55 (C2,6 methoxyphenyl), 139.97 (C4 hydroxyphenyl), 155.26 (C=N), 156.41 (C2 hydroxyphenyl), 156.86 (C4 methoxyphenyl), 178.06 (C=S) ppm. Anal. Calcd for C₁₇H₁₅N₃O₂S (325.38). Calculated: C, 62.75; H, 4.65; N, 12.91. Found: C, 62.51; H, 4.78; N, 13.08.

3.4. General Procedure for the Synthesis (E)-2-((3-Acetyl-5-(4-chlorophenyl)-2-thioxo-2,3-dihydro-1H-imidazol-1-ylimino)methyl)phenyl Acetate (6)

A solution of compound **4b** (0.01 mol) in acetic anhydride (20 mL) was heated under reflux for 2 h, then cooled down and decanted into water. The reaction mixture was left for 24 h, and the precipitate formed was filtered off, washed with water and dried. Finally, the product was crystallized from benzene to give **6**.

Colorless crystals, yield 63%, m.p. 115–117 °C. IR (KBr) ν_{\max} : 3090 (arom.CH), 2934 (aliph.CH), 1766, 1696 (C=O), 1606 (C=N), 1521, 1484 (C=C), 1274 (C=S) cm^{-1} . $^1\text{H-NMR}$ (DMSO- d_6) δ : 2.08 (s, 3H, COCH₃), 2.54 (s, 3H, COCH₃), 7.29 (d, J = 8.1 Hz, 1H, arom.CH), 7.44 (t, J = 7.5 Hz, 1H, arom.CH), 7.52 (d, J = 8.5 Hz, 2H, arom.CH), 7.60 (t, 1H, arom.CH), 7.93 (d, J = 8.5 Hz, 2H, arom.CH), 8.10 (d, 1H, arom.CH), 8.15 (s, 1H, H-4 of imidazole ring), 8.99 (s, 1H, CH=N) ppm. $^{13}\text{C-NMR}$ (DMSO- d_6) δ : 20.02 (CH₃CO), 22.95 (CH₃CO), 114.59 (C4 imidazole), 124.04 (C3 acetoxyphenyl), 126.18 (C1 acetoxyphenyl), 127.10 (C5 acetoxyphenyl), 127.38 (C5 imidazole), 127.85 (C2,6 chlorophenyl), 129.34 (C3,5 chlorophenyl), 132.84 (C6 acetoxyphenyl), 133.05 (C4 acetoxyphenyl), 148.60 (C1 chlorophenyl), 148.80 (C4 chlorophenyl), 150.36 (C=N), 156.28 (C2 acetoxyphenyl), 169.50 (C=O), 172.13 (C=O), 172.53 (C=S) ppm. Anal. Calcd for C₂₀H₁₆ClN₃O₃S (413.88). Calculated: C, 58.04; H, 3.90; N, 10.15. Found: C, 58.22; H, 4.07; N, 9.93.

3.5. Biological Studies

3.5.1. Antitumor Activity against Three Cancer Cell Lines

Antitumor activity of the newly prepared imidazole compounds **4a–e** and **5** were carried out against MCF-7, HepG2, HCT-116, and MCF-10A using the MTT assay method. Cells at a density of 1×10^4 were seeded in 96-well plates at 37 °C for 48 h under 5% CO₂. After incubation, the cells were treated with different concentrations of the prepared molecules and incubated for 24 h. MTT dye was added at the end of 24 h of drug treatment and incubated for 4 h at 37 °C. Next, 100 μL of dimethyl sulfoxide was added to each well to dissolve the purple formazan formed. The color intensity of the formazan product, which represents the growth condition of the cells, is quantified using an ELISA plate reader at 570 nm. The experimental conditions were carried out with at least three replicates and the experiments were repeated at least three times.

3.5.2. Cell Cycle Analysis of Compounds **4d** and **5**

MCF-7 cells (2×10^5 /well) were harvested and washed twice in PBS. After that, cells were incubated at 37 °C and 5% CO₂. The medium was replaced with DMSO (1% v/v) containing the tested compounds, then incubated for 48 h, washed twice in PBS, fixed with 70% ethanol, rinsed again with PBS, and then stained with DNA fluorochrome PI for 15 min at 37 °C. DNA content was analyzed by flow cytometry on a FACS Calibur flow cytometer (Becton and Dickinson, Heidelberg, Germany).

3.5.3. Annexin V FITC/PI Apoptosis Detection Staining Assay

Apoptosis in MCF-7 cells was investigated using fluorescent Annexin V-FITC/PI detection kit by flow cytometry assay. Briefly, MCF-7 cells (2×10^5) after incubation for 12 h. Cells were treated with compounds **4d** and **5** at their IC₅₀ concentration for 48 h, then the cells were harvested and stained with Annexin V-FITC/PI dye for 15 min in the dark at 37 °C. Flow cytometry analyses were performed using a FACS Calibur flow cytometer (Becton and Dickinson, Heidelberg, Germany).

3.5.4. In Vitro VEGFR-2 Kinase Assay

VEGFR-2 inhibitory activity for compounds **4d**, **5**, and erlotinib was evaluated using human VEGFR-2 ELISA kits according to the manufacturer's instructions. A total of 100 μL of standard solution and tested molecules were pipetted into the 96-wells and VEGFR-2 was bound to the wells by the immobilized antibody. The wells were washed and biotinylated antihuman VEGFR-2 antibody was added. After washing away unbound biotinylated

antibody, 100 μ L of conjugated streptavidin solution was pipetted into the wells. After washing, 100 μ L of TMB substrate solution was added to the wells for 30 min at 37 °C. Stop solution (50 μ L) was added, and the intensity of the color was measured immediately at 450 nm.

3.5.5. In Vitro B-Raf Kinase Assay

RAF inhibitory activity for compounds **4d**, **5**, and erlotinib was evaluated using human B-RAF ELISA kits according to the manufacturer's instructions. Next, 100 μ L of standard solution and tested molecules were pipetted into the 96-wells and B-RAF was bound to the wells by the immobilized antibody. The wells were washed and biotinylated antihuman B-Raf antibody was added. After washing away unbound biotinylated antibody, 100 μ L of conjugated streptavidin solution was pipetted into the wells. After washing, 100 μ L of TMB substrate solution was added to the wells for 30 min at 37 °C. Stop solution (50 μ L) was added, and the intensity of the color is measured immediately at 450 nm.

3.6. Molecular Docking Study

A molecular docking study was performed using the MOE software program (MOE 2009.10). The VEGFR-2 crystal structure (PDB code: 3U6J) was obtained from a protein data bank (Supplementary Materials).

4. Conclusions

In conclusion, a novel series of imidazoles bearing arylidene amino substituents at the *N*-1 position were synthesized in order to investigate their anticancer activity. The structure of the prepared imidazole derivatives was confirmed utilizing spectral data such as IR, ¹H-NMR, and ¹³C-NMR along with elemental analyses. The prepared imidazoles molecules were screened for their cytotoxic activity against three cancer cell lines namely, MCF-7 breast cancer, HepG2 liver cancer, and HCT-116 colon cancer cell lines. Compound **5** was the most potent of all against the three cell lines. DNA flow cytometric analysis showed that, compounds **4d** and **5** exhibit pre-G1 apoptosis and cell cycle arrest at the G2/M phase. The results of the VEGFR-2 and B-Raf kinase inhibition assays revealed that compounds **4d** and **5** displayed good inhibitory activity compared with the reference drug erlotinib. Finally, imidazole compounds **4d** and **5** could serve as lead chemical entities for further structural optimization as anticancer agents.

Supplementary Materials: Figure S1: ¹H-NMR spectrum of compound **3a**, Figure S2: ¹³C-NMR spectrum of compound **3a**, Figure S3: ¹H-NMR spectrum of compound **3b**, Figure S4: ¹³C-NMR spectrum of compound **3b**, Figure S5: ¹H-NMR spectrum of compound **3c**, Figure S6: ¹³C-NMR spectrum of compound **3c**, Figure S7: ¹H-NMR spectrum of compound **3d**, Figure S8: ¹³C-NMR spectrum of compound **3d**, Figure S9: ¹H-NMR spectrum of compound **4a**, Figure S10: ¹³C-NMR spectrum of compound **4a**, Figure S11: ¹H-NMR spectrum of compound **4b**, Figure S12: ¹³C-NMR spectrum of compound **4b**, Figure S13: ¹H-NMR spectrum of compound **4c**, Figure S14: ¹³C-NMR spectrum of compound **4c**, Figure S15: ¹H-NMR spectrum of compound **4d**, Figure S16: ¹³C-NMR spectrum of compound **4d**, Figure S17: ¹H-NMR spectrum of compound **4e**, Figure S18: ¹³C-NMR spectrum of compound **4e**, Figure S19: ¹H-NMR spectrum of compound **5**, Figure S20: ¹³C-NMR spectrum of compound **5**, Figure S21: ¹H-NMR spectrum of compound **6**, Figure S22: ¹³C-NMR spectrum of compound **6**.

Author Contributions: Conceptualization, A.H.A.A., E.-S.H.E.-S., M.A.M.T. and I.Z.; methodology, E.E.M.T., M.A.M.T. and A.H.A.A.; data curation, E.F., O.A.A.A., A.H.A.A. and I.Z.; software, I.Z., A.H.A.A., E.F. and O.A.A.A.; resources, I.Z., A.H.A.A., E.F., O.A.A.A. and E.E.M.T.; supervision, A.H.A.A., E.-S.H.E.-S., M.A.M.T.; funding acquisition, E.F. and O.A.A.A.; original draft preparation, A.H.A.A., I.Z., E.F. and O.A.A.A.; Writing, review, and editing, all authors. All authors have read and agreed to the published version of the manuscript.

Funding: Taif University Researchers Supporting Project number (TURSP-2020/220), Taif University, Taif, Saudi Arabia.

Data Availability Statement: MDPI Research Data Policies” at <https://www.mdpi.com/ethics>.

Acknowledgments: Taif University Researchers Supporting Project number (TURSP-2020/220), Taif University, Taif, Saudi Arabia.

Conflicts of Interest: The authors declare no conflict of interest.

Sample Availability: Samples of the compounds not available from the authors.

References

1. Li, Q.; Zhang, Z.; Fan, Y.; Zhang, Q. Epigenetic Alterations in Renal Cell Cancer with TKIs Resistance: From Mechanisms to Clinical Applications. *Front. Genet.* **2021**, *11*, 562868. [[CrossRef](#)] [[PubMed](#)]
2. Fane, M.; Weeraratna, A.T. How the ageing microenvironment influences tumour progression. *Nat. Rev. Cancer* **2020**, *20*, 89–106. [[CrossRef](#)]
3. Bianchi, J.J.; Zhao, X.; Mays, J.C.; Davoli, T. Not all cancers are created equal: Tissue specificity in cancer genes and pathways. *Curr. Opin. Cell Biol.* **2020**, *63*, 135–143. [[CrossRef](#)] [[PubMed](#)]
4. Hou, Y.; Shang, C.; Wang, H.; Yun, J. Isatin–azole hybrids and their anticancer activities. *Arch. Pharm.* **2019**, *353*, 1900272. [[CrossRef](#)] [[PubMed](#)]
5. Guo, H.; Diao, Q.-P. 1, 3, 5-Triazine-azole Hybrids and their Anticancer Activity. *Curr. Top. Med. Chem.* **2020**, *20*, 1481–1492. [[CrossRef](#)]
6. Ali, E.M.H.; Abdel-Maksoud, M.S.; Ammar, U.M.; Mersal, K.I.; Yoo, K.H.; Jooryeong, P.; Oh, C.-H. Design, synthesis, and biological evaluation of novel imidazole derivatives possessing terminal sulphonamides as potential BRAFV600E inhibitors. *Bioorg. Chem.* **2021**, *106*, 104508. [[CrossRef](#)]
7. Yang, Y.-Q.; Chen, H.; Liu, Q.-S.; Sun, Y.; Gu, W. Synthesis and anticancer evaluation of novel 1H-benzo[d]imidazole derivatives of dehydroabietic acid as PI3K α inhibitors. *Bioorg. Chem.* **2020**, *100*, 103845. [[CrossRef](#)]
8. Singh, I.; Luxami, V.; Paul, K. Synthesis of naphthalimide-phenanthro[9,10-d]imidazole derivatives: In vitro evaluation, binding interaction with DNA and topoisomerase inhibition. *Bioorg. Chem.* **2020**, *96*, 103631. [[CrossRef](#)] [[PubMed](#)]
9. Biskupiak, J.E.; Grierson, J.R.; Rasey, J.S.; Martin, G.V.; Krohn, K.A. Synthesis of an (iodovinyl)misonidazole derivative for hypoxia imaging. *J. Med. Chem.* **1991**, *34*, 2165–2168. [[CrossRef](#)] [[PubMed](#)]
10. Franchetti, P.; Marchetti, S.; Cappellacci, L.; Yalowitz, J.A.; Jayaram, H.N.; Goldstein, B.M.; Grifantini, M. ChemInform Abstract: A New C-Nucleoside Analogue of Tiazofurin: Synthesis and Biological Evaluation of 2- β -D-Ribofuranosylimidazole-4-carboxamide (Imidazofurin). *Bioorg. Med. Chem. Lett.* **2001**, *32*, 67–69. [[CrossRef](#)]
11. Cui, B.; Zheng, B.L.; He, K.; Zheng, Q.Y. Imidazole Alkaloids from *Lepidium meyenii*. *J. Nat. Prod.* **2013**, *66*, 1101–1103. [[CrossRef](#)]
12. Zeng, L.; Wu, Q.; Wang, T.; Li, L.-P.; Zhao, X.; Chen, K.; Qian, J.; Yuan, L.; Xu, H.; Mei, W.-J. Selective stabilization of multiple promoter G-quadruplex DNA by using 2-phenyl-1H-imidazole-based tanshinone IIA derivatives and their potential suppressing function in the metastatic breast cancer. *Bioorg. Chem.* **2021**, *106*, 104433. [[CrossRef](#)] [[PubMed](#)]
13. Chavda, J.; Bhatt, H. Systemic review on B-RafV600E mutation as potential therapeutic target for the treatment of cancer. *Eur. J. Med. Chem.* **2020**, *206*, 112675. [[CrossRef](#)]
14. Johnson, J.C.; Martinez, O.; Honko, A.N.; Hensley, L.E.; Olinger, G.G.; Basler, C.F. Pyridinyl imidazole inhibitors of p38 MAP kinase impair viral entry and reduce cytokine induction by Zaire ebolavirus in human dendritic cells. *Antivir. Res.* **2014**, *107*, 102–109. [[CrossRef](#)] [[PubMed](#)]
15. Zaki, I.; Ramadan, H.M.; El-Sayed, E.S.; Abd El-Moneim, M. Design, synthesis, and cytotoxicity screening of new synthesized imidazolidine-2-thiones as VEGFR-2 enzyme inhibitors. *Arch. Pharm.* **2020**, *353*, 2000121. [[CrossRef](#)] [[PubMed](#)]
16. Bellina, F.; Cauteruccio, S.; Rossi, R. Synthesis and biological activity of vicinal diaryl-substituted 1H-imidazoles. *Tetrahedron* **2007**, *63*, 4571–4624. [[CrossRef](#)]
17. Inman, G.J.; Nicolás, F.J.; Callahan, J.F.; Harling, J.D.; Gaster, L.M.; Reith, A.D.; Laping, N.J.; Hill, C.S. SB-431542 Is a Potent and Specific Inhibitor of Transforming Growth Factor- β Superfamily Type I Activin Receptor-Like Kinase (ALK) Receptors ALK4, ALK5, and ALK7. *Mol. Pharmacol.* **2002**, *62*, 65–74. [[CrossRef](#)] [[PubMed](#)]
18. Agarwal, R.K.; Singh, L.; Sharma, D.K. Synthesis, Spectral, and Biological Properties of Copper(II) Complexes of Thiosemicarbazones of Schiff Bases Derived from 4-Aminoantipyrine and Aromatic Aldehydes. *Bioinorg. Chem. Appl.* **2006**, *2006*, 1–10. [[CrossRef](#)] [[PubMed](#)]
19. Hassan, M.; Ghaffari, R.; Sardari, S.; Farahani, Y.F.; Mohebbi, S. Discovery of novel isatin-based thiosemicarbazones: Synthesis, antibacterial, antifungal, and antimycobacterial screening. *Res. Pharm. Sci.* **2020**, *15*, 281–290. [[CrossRef](#)]
20. Abdelhameid, M.K.; Zaki, I.; Mohammed, M.R.; Mohamed, K.O. Design, synthesis, and cytotoxic screening of novel azole derivatives on hepatocellular carcinoma (HepG2 Cells). *Bioinorg. Chem.* **2020**, *101*, 103995. [[CrossRef](#)] [[PubMed](#)]
21. Roskoski, R. Properties of FDA-approved small molecule protein kinase inhibitors: A 2021 update. *Pharmacol. Res.* **2019**, *144*, 19–50. [[CrossRef](#)] [[PubMed](#)]
22. Norman, M.H.; Liu, L.; Lee, M.; Xi, N.; Fellows, I.; D’Angelo, N.D.; Dominguez, C.; Rex, K.; Bellon, S.F.; Kim, T.S. Structure-Based Design of Novel Class II c-Met Inhibitors: 1. Identification of Pyrazolone-Based Derivatives. *J. Med. Chem.* **2012**, *55*, 1858–1867. [[CrossRef](#)] [[PubMed](#)]